

# Aspects Regarding the Unidirectional Two-Port Circuits Implemented by Means of Electronic Gytrators

Gabriela TONȚ<sup>1</sup>, Radu Adrian MUNTEANU<sup>2</sup>, Dan George TONȚ<sup>1</sup>, Dan IUDEAN<sup>2</sup>

<sup>1</sup>University of Oradea, 410087, Romania,

<sup>2</sup>Technical University Cluj Napoca, 400020, Romania  
gtont@uoradea.ro

**Abstract**—The paper investigates the behavior of unidirectional two-port equivalent circuit composed of an electronic gyrator with Antoniou operational amplifier and a reciprocal two-port built by a transversal resistance ( $R_T$ ). From the analysis of two-port equations standpoint, by correct choice of circuit conductance, the two-port can operate as an ideal or a lossy gyrator. Due to the interest in practical aspects of energy transfer from one terminal to other, an analysis of the two-port parameters for the unidirectional circuit diagram is performed. The validity of the tested circuit results obtained analytically and through numerical simulation PSpice has been verified experimentally, in two cases, with equal and different transfer conductance.

**Index Terms**—gyrator, operational amplifiers, simulation, transfer functions, two-port.

## I. INTRODUCTION

A two-port circuit is unidirectional if the transfer of electromagnetic energy has a single direction [1]. The unidirectional condition from port 11' to 22' implies that the no-load impedance ( $Z_{l0}$ ), and short circuit impedance ( $Z_{lk}$ ), at port 11' are equal ( $Z_{l0}=Z_{lk}$ ), the energy being transferred from input port 11' to output port 22'. Taking into account the unidirectional condition, the no-load transfer impedance ( $Z_{l2}$ ), and the short circuit transfer admittance ( $Y_{l2}$ ) are zero ( $Z_{l2}=Y_{l2}=0$ ), the voltage ( $U_1$ ), and current ( $I_1$ ), at port 11' are independent on the output voltage ( $U_2$ ) and current ( $I_2$ ), at port 22' [2]. In this case, the energy transfer in reverse direction doesn't take place (see Figure 1).

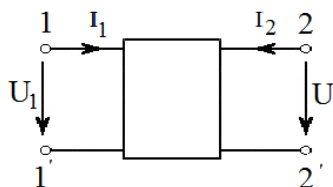


Figure 1. Graphical representation of a two-port

This behaviour of the two-port equivalent diagram can be symbolized as  $1^* \rightarrow 2$ , respectively  $2 \rightarrow 1^*$ , where the asterisk shows that the circuit is supplied from port 11' to port 22' [3].

Taking into account the considerations above, the unidirectionality condition can be written as in relationship (1), where (e) is the index for the equivalent two-port circuit:

$$R_{e12} = G_{e12} = 0 \quad (1)$$

In terms of structure, a unidirectional two-port can be

implemented through an appropriate combination of a gyrator with a reciprocal two-port.

In unidirectional two-port, in which the energy is transferred from ports 11' to 22' only, the determinant of chain matrix  $A$  is null,  $\det[A]=0$ . In this equivalent circuit, the input impedance ( $Z_{e1}$ ) is independent of the receptor impedance ( $Z_R$ ). This implies that the no-load impedance ( $Z_{e10}$ ), and short circuit impedance ( $Z_{e1k}$ ) have equal values ( $Z_{e10}=Z_{e1k}$ ) [4-7].

Indeed, the equivalent input impedance of a two-port can be decomposed twofold as in relationship below:

$$\begin{aligned} Z_{e1} &= \frac{A_{11}Z_R + A_{12}}{A_{21}Z_R + A_{22}} = \frac{A_{11}}{A_{21}} - \frac{\det[A]}{A_{21}(A_{21}Z_R + A_{22})} = \\ &= Z_{e10} - \frac{\det[A]}{A_{21}(A_{21}Z_R + A_{22})}. \end{aligned} \quad (2)$$

or

$$\begin{aligned} Z_{e1} &= \frac{A_{11}Z_R + A_{12}}{A_{21}Z_R + A_{22}} = \frac{A_{12}}{A_{22}} + \frac{Z_R \det[A]}{A_{22}(A_{21}Z_R + A_{22})} = \\ &= \frac{1}{Y_{e1k}} + \frac{Z_S \det[A]}{A_{22}(A_{21}Z_R + A_{22})}. \end{aligned}$$

It is noticeable that, if  $\det[A]=0$  it results the equality of equivalent impedances ( $Z_{e1}=Z_{e10}=Z_{e1k}$ ), respectively, the equivalent two-port transfer impedance and transfer admittance are null ( $Z_{e12}=Y_{e12}=0$ ). These equations are the characteristics of unidirectional two-port [8].

## II. ANALYSIS OF A GYRATOR BUILT WITH OPERATIONAL AMPLIFIERS

An example of gyrator with operational amplifiers is shown below, in Figure 2 [9-10].

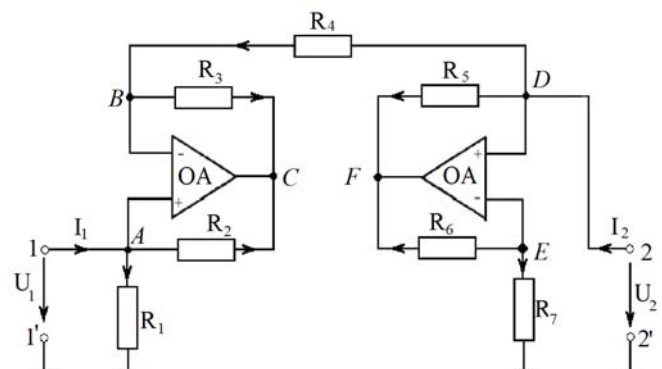


Figure 2. Antoniou Gyrator with operational amplifiers

Assuming that the open loop gain is infinite for the two operational amplifiers, the equations of Antoniou gyrator can be detracted as follows:

$$I_1 = U_1 \left( G_1 - \frac{G_2 G_4}{G_3} \right) + U_2 \frac{G_2 G_4}{G_3} \quad (3)$$

$$I_2 = -U_1 G_4 + U_2 \left( G_4 - \frac{G_5 G_7}{G_6} \right) \dots$$

The two-port parameters ensuing from equations (3) have the following expressions:  $G_{11}=G_1-G_2 \cdot G_4 / G_3$ ;  $G_{12}=G_2 \cdot G_4 / G_3$ ;  $G_{21}=-G_4$ ;  $G_{22}=G_4-G_5 \cdot G_7 / G_6$ , where ( $G_{11}$ ) and ( $G_{22}$ ) are the conductance in short circuit to terminals 11' respectively 22', ( $G_{12}$ ) and ( $G_{21}$ ) are the transfer conductance in short circuit. Due to the fact that the product of transfer conductance is negative ( $G_{12}G_{21}<0$ ), it can be concludes that the analyzed schematics has a gyrator like behaviour [11].

By choosing certain values of two-port parameters which depend on conductance ( $G_1...G_7$ ), the obtained gyrators can be either ideal or with losses [12-13]. Depending on chosen values of conductance ( $G_1...G_7$ ), the resulting transfer conductance can be equal ( $|G_{12}|=|G_{21}|$ ), or unequal ( $|G_{12}| \neq |G_{21}|$ ). In order to obtain an ideal gyrator, the conductance in short circuit from the terminals 11' and 22' have to be zero ( $G_{11}=G_{22}=0$ ), which can be expressed as ( $G_1 \cdot G_3 = G_2 \cdot G_4$ ) and ( $G_4 \cdot G_6 = G_5 \cdot G_7$ ).

The boundary condition for ideal gyrators can be meet, either by choosing an equal conductance in a circuit ( $G_1=G_2=...=G_7=G$ ), in which case the transfer conductance will be equal in numerical value ( $G_{12}=G$  and  $G_{21}=-G$ ), or by choosing certain values for the two conductance groups ( $G_1=G_2=G_6=G_7=G'$  and  $G_3=G_4=G''$ ), in which case the transfer parameters will have different numerical values ( $G_{12}=G'$  and  $G_{21}=-G''$ ).

Similarly, the selection of conductance values in circuit can be examined in order of obtaining a gyrator which is not ideal, ( $G_{11} \neq 0$ ,  $G_{22} \neq 0$ ). For example, if it is selected the conductance to have the same values ( $G_2=G_3=G_5=G_7=G$ ) and ( $G_1, G_4, G_6$ ) are chosen to meet the inequality ( $G_1 > G_4 > G_6$ ), the conductance ( $G_{11}$ ) and ( $G_{22}$ ) will be positive and non-zero, and the transfer two-port parameters in short circuit will have equal numerical values ( $G_{12}=G_4$ ,  $G_{21}=-G_4$ ).

The ideals gyrators are lossless due to the fact that the losses corresponding to parameters ( $G_{11}$ ) and ( $G_{22}$ ) are zero, which is advantageous for the energy transfer between the terminals.

The option of building ideal gyrators with operational amplifiers should be specially mentioned because this possibility doesn't exist when the circuit is built with Hall gyrators, given their natural lossy behaviour [14-15].

### III. THE ANALYSIS OF AN UNIDIRECTIONAL CIRCUIT

In regards to the possibility of obtaining a unidirectional two-port circuit, in the literature, two main circuit diagrams are mentioned (Figure 3a and Figure 3b).

In Figure 3a, the reciprocal two-port component is represented by longitudinal resistances ( $R_L$ ) and ( $R'_L$ ).

In Figure 3b the reciprocal two-port component is built by a T-two-port. Since the resistances ( $r$ ) and ( $r'$ ) do not

actually occur in the unidirectionality condition, they could be omitted out of the circuit, therefore from the reciprocal two-port in T only the transversal resistance ( $R_T$ ) would remain.

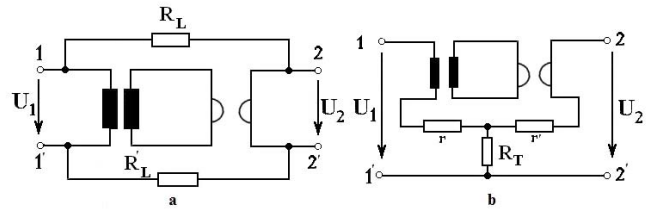


Figure 3. Unidirectional two-port with longitudinal resistances (3a) and transversal resistance (3 b)

The circuit diagram with equal longitudinal resistances ( $R_L=R'_L$ ) is usually mentioned when the gyrator is based on the Hall Effect (see Figure 4).

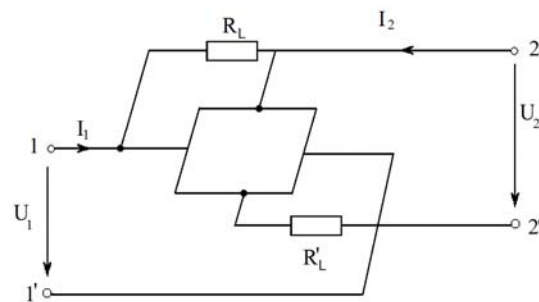


Figure 4. A unidirectional two-port gyrator with Hall gyrator

By introducing an ideal transformer into a unidirectional circuit diagram, the gyrator is galvanically separated from the reciprocal two-port [16-18]. In addition, the two-port components of the unidirectional circuit can be regarded as two-port in the equivalent circuit, which simplifies the analysis [19-20].

The resistance matrix ( $[R]$ ) of a Hall gyrator is presented in the equation (4), below, where ( $B$ ) is magnetic induction, and ( $S_0$ ) is no-load sensitivity of Hall gyrator:

$$[R] = \begin{bmatrix} R_{11} & R_{12} \\ R_{21} & R_{22} \end{bmatrix} = \begin{bmatrix} R_{10} & S_0 B \\ -S_0 B & R_{20} \end{bmatrix} \quad (4)$$

Having analytically expressed the resistance matrix  $[R]$ , the conductance matrix of the Hall gyrator  $[G]$  can be written under the form of relationship (5), where it is taken into account that the product of transfer resistances is lesser than zero,  $R_{12} \cdot R_{21} < 0$ :

$$[G] = \frac{1}{R_{11}R_{22} + |R_{12}R_{21}|} \begin{bmatrix} R_{20} & -S_0 B \\ S_0 B & R_{10} \end{bmatrix} \quad (5)$$

The equivalent conductance matrix  $[G_e]$  is obtained by summing the conductance matrices of the two-port components ( $[G_e]=[G]+[G_L]$ ) as it is developed in the equation (6), where  $[G_L]$  is the conductance matrix of the reciprocal two-port longitudinal resistances [21-24]:

$$[G_e] = \begin{bmatrix} G_{e11} & G_{e12} \\ G_{e21} & G_{e22} \end{bmatrix} = \begin{bmatrix} G_{11} & G_{12} \\ G_{21} & G_{22} \end{bmatrix} + \frac{1}{2} \begin{bmatrix} \frac{1}{R_L} & \frac{1}{R_L} \\ \frac{1}{R_L} & \frac{1}{R_L} \end{bmatrix} \quad (6)$$

$$[G_e] = \begin{bmatrix} \frac{R_{20}}{R_{10}R_{20} + (S_0B)^2} + \frac{1}{2R_L} & -\frac{S_0B}{R_{10}R_{20} + (S_0B)^2} + \frac{1}{2R_L} \\ \frac{S_0B}{R_{10}R_{20} + (S_0B)^2} + \frac{1}{2R_L} & \frac{R_{10}}{R_{10}R_{20} + (S_0B)^2} + \frac{1}{2R_L} \end{bmatrix}$$

The unidirectionality condition given by the transfer conductance of equivalent circuit equal with zero ( $G_{e12}=0$ ) is met if the longitudinal resistance is expressed as in equation (7):

$$R_L = \frac{R_{10}R_{20} + (S_0B)^2}{2(S_0B)} \quad (7)$$

Regarding the Hall gyrator as part of a unidirectional circuit diagram, it should be mentioned that, because of the large losses in Hall plate, the direct attenuation in these circuits is relatively high, thus the interest in them is mostly theoretical [25-27].

The aim of the paper is to analyze the problem of unidirectional circuit built with a gyrator with operational amplifiers as an anti-reciprocal element. In the current literature, this solution was not reported.

Referring specifically to an Antoniou gyrator with operational amplifiers, from the circuit equations it results that the conductance matrix ( $[G]$ ), is defined as in equation (8):

$$[G] = \begin{bmatrix} G_1 - \frac{G_2G_4}{G_3} & \frac{G_2G_4}{G_3} \\ -G_4 & G_4 - \frac{G_5G_7}{G_6} \end{bmatrix} \quad (8)$$

By properly sizing the circuit and selecting all resistances to equal value, for instance ( $R$ ), a theoretical ideal gyrator can be obtained with the following conductance parameters:  $G_{11}=G_{22}=0$ ,  $G_{12}=G$ , and  $G_{21}=-|G_{21}|=-G$ , where  $G=1/R$ . In this case, in order to build the unidirectional circuit diagram are serially connected the operational amplifiers gyrator with a transversal resistance ( $R_T$ ), (see Figure 5) [28-30].

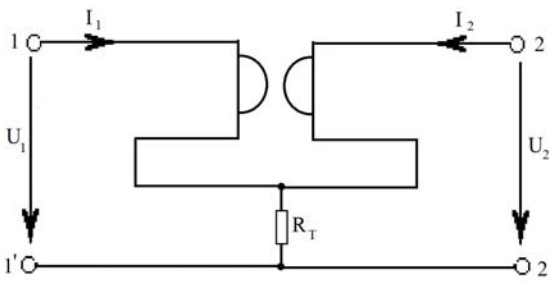


Figure 5. A unidirectional two-port gyrator with transversal resistance ( $R_T$ )

By summing the resistance matrices of the serial two-ports, the equivalent resistance matrix  $[R_e]$  is obtained and it can be expressed as in the equation (9), below:

$$[R_e] = \begin{bmatrix} R_{e10} & R_{e12} \\ R_{e21} & R_{e20} \end{bmatrix} = \begin{bmatrix} R_{10} & -|R_{12}| \\ R_{21} & R_{20} \end{bmatrix} + \begin{bmatrix} R_T & R_T \\ R_T & R_T \end{bmatrix} = \begin{bmatrix} R_{10} + R_T & -|R_{12}| + R_T \\ R_{21} + R_T & R_{20} + R_T \end{bmatrix} \quad (9)$$

This relationship (9) is simplified if the gyrator is ideal ( $R_{10}=0$ ,  $R_{20}=0$ ). The circuit can become unidirectional if is satisfied the condition expressed as in equation (10):

$$R_T = |R_{12}| \quad (10)$$

By knowing the equivalent resistance matrix ( $[R_e]$ ), the equivalent conductance matrix ( $[G_e]$ ) can be computed as in relationship (11), where the denoted  $\det[R_e]$  is the determinant of the equivalent matrix (12):

$$[G_e] = \frac{1}{\det[R_e]} \begin{bmatrix} R_{e20} & -R_{e12} \\ -R_{e21} & R_{e10} \end{bmatrix} \quad (11)$$

$$\det[R_e] = (R_{10} + R_T) \cdot (R_{20} + R_T) - (R_T - |R_{12}|) \cdot (R_{21} + R_T) \quad (12)$$

The short circuit conductance of the equivalent two-port supplied at port 11' can be written under the form of relationship (13):

$$G_{e1k} = \frac{R_{e22}}{\det[R_e]} = \frac{R_{20} + R_T}{\det[R_e]} \quad (13)$$

If  $R_T=|R_{12}|$ , the equation (13) is given by the following equation:

$$G_{e1k} = \frac{R_{20} + R_T}{(R_{10} + R_T) \cdot (R_{20} + R_T)} = \frac{1}{R_{e10}} = G_{e10} \quad (14)$$

This equation verifies the equality of the equivalent conductance ( $G_{e1k}=G_{e10}$ ). The equivalent unidirectional circuit parameters being known, the transmission constant ( $g_{1c}$ ), can be determined. In this case, the transmission constant is equal to the attenuation constant ( $a_{1c}$ ), due to the resistive nature of the circuit, therefore the common equation  $a_{1c} = \ln 2\sqrt{R_{e10}R_{e20}} / R_{e21}$  is applied. Conversely, the attenuation constant of a unidirectional electronic circuit is infinite, ( $a_{1c} = \infty$ ) because of the fact that the transfer equivalent resistance ( $R_{e12}$ ), which is present in the denominator of the relationship  $a_{2c} = \ln 2\sqrt{R_{e10}R_{e20}} / R_{e12}$ , is zero [31-32].

#### IV. THE DEVELOPMENT OF THE TWO-PORT UNIDIRECTIONAL CIRCUITS WITH OPERATIONAL AMPLIFIERS THROUGH NUMERICAL SIMULATION WITH PSpICE

Considering a unidirectional circuit built with operational amplifiers and a transversal resistance, structure which meets the conditions:  $G_{21}=-|G_{21}|<0$  and  $G_{12}>0$ , derived from gyrator equations (3), the gyrator circuit can be calculated to have a passive behaviour. The schematic of Antoniou gyrator with operational amplifiers was build using components parts from the PSpice Library.

The simulation profile was set as in the cases a and b, where it was taken into account the relationships resulting from the resistance matrix transferred to conductance matrix of ideal two-port,  $R_{12}=-1/|G_{21}|$  and  $R_{21}=-1/|G_{12}|$ :

- case a:  $G_{12}=1$  mS;  $G_{21}=-1$  mS, respectively  $R_{12} = -1$  k $\Omega$ ;  $R_{21} = 1$  k $\Omega$ ;
- case b:  $G_{12}=2$  mS;  $G_{21}=-1$  mS, respectively  $R_{12} = -1$  k $\Omega$ ;  $R_{21} = 0.5$  k $\Omega$ ,

The case (a) corresponds to a first set of equal conductance, namely: ( $G_1=G_2=...=G_7=G$ ), case where, the gyrator equations (3) lead to two-port parameters  $G_{11}=G_{22}=0$  and  $G_{12}=G_{21}=G$ , specific to ideal gyrator. The two-port resistance parameters corresponding to conductance are:  $R_{11}=R_{22}=0$ ,  $R_{21}=-R_{12}=R$ , where  $R_{12}=1/G$ . Setting the voltage  $U=1V$ , and the frequency  $f=950Hz$ , the

results obtain by running the simulation in case  $R=G^{-1}=1$  k $\Omega$ , are presented in Table I. The two-port parameters of the ideal gyrator are obtained analytically (column one), through PSpice simulation (column two), and experimentally (column three).

TABLE I. THE VALUES TWO-PORT PARAMETERS OF IDEAL GYRATOR, IN THE CASE A

Analytical	PSpice	Experimental f=950Hz, U=1V	Obs.
$G_{11}=0$	$G_{11}=0,0007 \cdot 10^{-3}$	$G_{11}=0,18 \cdot 10^{-3}$	Ideal Gyrator $ G_{12} = G_{21} $
$G_{12}=1 \cdot 10^{-3}$	$G_{12}=1 \cdot 10^{-3}$	$G_{12}=0,99 \cdot 10^{-3}$	
$G_{21}=-1 \cdot 10^{-3}$	$G_{21}=-1 \cdot 10^{-3}$	$G_{21}=-0,88 \cdot 10^{-3}$	
$G_{22}=0$	$G_{22}=0,0005 \cdot 10^{-3}$	$G_{22}=0,16 \cdot 10^{-3}$	
$R_{11}=0$	$R_{11}=0,0005 \cdot 10^3$	$R_{11}=0,18 \cdot 10^3$	
$R_{12}=-1 \cdot 10^3$	$R_{12}=-1 \cdot 10^3$	$R_{12}=-1,1 \cdot 10^3$	
$R_{21}=1 \cdot 10^3$	$R_{21}=1 \cdot 10^3$	$R_{21}=0,98 \cdot 10^3$	
$R_{22}=0$	$R_{22}=0,0007 \cdot 10^3$	$R_{22}=0,2 \cdot 10^3$	

In the case b, the two-ports parameters are  $R_{11}=R_{22}=0$  and  $R_{12}=-R''$ ,  $R_{21}=R'$ , where  $R'=1/G'$ ,  $R''=1/G''$ .

The first column of Table II contains two-port parameters values consequential to the calculation, the second column includes the parameters obtained experimentally, and the third one contains data gathered through PSpice simulation in sinusoidal steady-state at 1kHz,  $R^1=R''=2$ k $\Omega$  and  $R''=3$ k $\Omega$ .

TABLE II. THE VALUE OF TWO-PORT PARAMETERS OF AN IDEAL GYRATOR, IN THE CASE B

Analytical	PSpice	Experimental f=950Hz, U=1V	Obs.
$G_{11}=0$	$G_{11}=0,0014 \cdot 10^{-3}$	$G_{11}=0,3 \cdot 10^{-3}$	Ideal Gyrator $ G_{12} =2 G_{21} $
$G_{12}=2 \cdot 10^{-3}$	$G_{12}=2 \cdot 10^{-3}$	$G_{12}=1,99 \cdot 10^{-3}$	
$G_{21}=-1 \cdot 10^{-3}$	$G_{21}=-1 \cdot 10^{-3}$	$G_{21}=-0,89 \cdot 10^{-3}$	
$G_{22}=0$	$G_{22}=0,0005 \cdot 10^{-3}$	$G_{22}=0,12 \cdot 10^{-3}$	
$R_{11}=0$	$R_{11}=0,0002 \cdot 10^3$	$R_{11}=0,07 \cdot 10^3$	
$R_{12}=-1 \cdot 10^3$	$R_{12}=-1 \cdot 10^3$	$R_{12}=-1,09 \cdot 10^3$	
$R_{21}=0,5 \cdot 10^3$	$R_{21}=0,5 \cdot 10^3$	$R_{21}=0,49 \cdot 10^3$	
$R_{22}=0$	$R_{22}=0,0007 \cdot 10^3$	$R_{22}=0,19 \cdot 10^3$	

For the two-port transfer parameters ( $G_{12}$ ,  $G_{21}$  and  $R_{12}$ ,  $R_{21}$ ), the same values were obtained experimentally as analytically and in numerical simulation, whereas the parameters defined at the ports ( $G_{11}$ ,  $G_{22}$  and  $R_{11}$ ,  $R_{22}$ ), obtained through PSpice simulation are not null. They are however negligible compared with the transfer parameters, being approximately  $10^{-3}$  times lower. These values correspond, in fact, to an ideal gyrator. Therefore, it can be conclude that, when the assumptions detailed above are taken into account, the essential features of the analyzed circuit are characteristic for the ideal gyrator.

Modifying, within certain limits the working frequency, could be regarded as a slight change of the parameters values defined at ports, but negligible compared to the transfer parameters. Consequently, the next step is to calculate the input equivalent resistance in no-load regime ( $R_{e10}$ ), based on subsequently on calculating the input conductance in short circuit ( $G_{e1k}$ ), respectively, the equivalent resistance in short circuit ( $R_{e1k}=1/G_{e1k}$ ). This reasoning leads to the equation (15), where it is taken into account that  $R_{12}=-|R_{12}|$  and  $R_{21}=|R_{21}|$ :

$$R_{e1k} = -(R_{12} + R_{21}) - \frac{R_{12}R_{21}}{R_T} = (|R_{12}| - |R_{21}|) + \frac{|R_{12}R_{21}|}{R_T} \quad (15)$$

For both referred cases, (a) and (b), the equivalent resistance expressions ( $R_{e1k}$ ), become as follows:

case a:  $R_{e1k}=1/R_T$

case b:  $R_{e1k}=0.5(1+1/R_T)$

Based on these equations, the graphic dependence between the equivalent resistance in short circuit ( $R_{e1k}$ ), and transversal resistance ( $R_T$ ), for the two cases (a, b) can be visualized.

### V. EXPERIMENTAL VERIFICATION UNIDIRECTIONAL CIRCUIT WITH OPERATIONAL AMPLIFIERS

To experimentally verify these results, the authors made a unidirectional circuit based on schematic from Figure 5 using Antoniou gyrator with operational amplifiers type AD712. Basically, the electronic assembly represents the cases (a) and (b) previously analyzed through calculation and numerical simulation based on PSpice. In order to determine the resistance parameters experimental tests were conducted in no-load regime, at the frequency of 950Hz, and by applying 1V voltage. The values of resistors ( $R_1...R_7$ ), from Antoniou gyrator in the cases (a, b) are covered in Table III.

TABLE III. THE VALUES OF RESISTORS FROM ANTONIOU GYRATOR

Case	Variable for each case						
	$R_1$ [k $\Omega$ ]	$R_2$ [k $\Omega$ ]	$R_3$ [k $\Omega$ ]	$R_4$ [k $\Omega$ ]	$R_5$ [k $\Omega$ ]	$R_6$ [k $\Omega$ ]	$R_7$ [k $\Omega$ ]
a	1	1	1	1	1	1	1
b	0.5	0.5	1	1	1	2	2

The two-port transfer parameters of gyrator in no-load regime ( $R_{12}$ ,  $R_{21}$ ), determined by calculation and through experiments are summarized in Table IV, below.

TABLE IV. THE TWO-PORT TRANSFER RESISTANCES  $R_{12}$  AND  $R_{21}$  OF GYRATOR DETERMINED BOTH ANALYTICALLY AND THROUGH EXPERIMENTS FOR THE TWO CASES (A, B)

Case	$R_{12}$ [k $\Omega$ ]		$R_{21}$ [k $\Omega$ ]	
	Analytical	Experimental	Analytical	Experimental
a	-1	-1.08	1	0.98
b	-1	-1.09	0.5	0.49

The no-load regime resistance at the input port ( $R_{10}$ ) was determined experimentally on the basis of equivalent diagrams configuration for cases (a) and (b). The values obtained are  $R_{10} \approx 0.1$ k $\Omega$  for configuration in case (a), respectively,  $R_{10} \approx 0.7$ k $\Omega$  for case (b).

The deviations of the transfer parameter values in the no-load regime and the ones determined experimentally (see Table IV) are considered acceptable. Moreover, in this type of gyrator, the transfer resistance in no-load regime ( $R_{12}$ ) is negative, respectively, the transfer conductance is greater than zero ( $G_{12} > 0$ ), which means that, in order to obtain a unidirectional two-port circuit diagram, should be considered the circuit with transversal resistance.

The characteristics  $R_{e10}(R_T)$ , and  $R_{e1k}(R_T)$  are visually represented in Figure 6, from the data gathered in Table V.

TABLE V. EXPERIMENTAL VALUES OF THE EQUIVALENT RESISTANCE IN NO LOAD REGIME ( $R_{e10}$ ), AND THE EQUIVALENT RESISTANCE IN SHORT CIRCUIT ( $R_{e1k}$ ) DEPENDING ON THE TRANSVERSAL RESISTANCE ( $R_T$ ).

FOR CASE (A)					
$R_T$ [k $\Omega$ ]	U1 [V]	$I_{e10}$ [mA]	$I_{e1k}$ [mA]	$R_{e10}$ [k $\Omega$ ]	$R_{e1k}$ [k $\Omega$ ]
0.1	1.02	5.65	0.12	0.18	8.50
0.3	1.02	3.49	0.30	0.29	3.40

0.5	1.02	2.09	0.51	0.48	2.00
0.8	1.02	1.30	0.85	0.78	1.20
1	1.02	1.05	1.05	0.97	0.97
1.2	1.02	0.84	1.28	1.22	0.80
1.5	1.02	0.70	1.68	1.45	0.60

Table V comprises values of the equivalent resistances determined through experiments for case (a) operating in the no-load regime ( $R_{e10}$ ), and in short circuit ( $R_{e1k}$ ).

The transversal resistance ( $R_T$ ), for which the two-port circuit diagram becomes unidirectional corresponds to the intersection of the equivalent resistances characteristics  $R_{e10}(R_T)$ , and  $R_{e1k}(R_T)$ .

The graphic in Figure 6 demonstrates that this condition is met if  $R_T = 1k\Omega$ . The characteristics of equivalent resistances values obtained experimentally are  $R_{e10} = R_{e1k} = 0.97k\Omega$ , for the transfer resistance  $R_T = 1k\Omega$ .

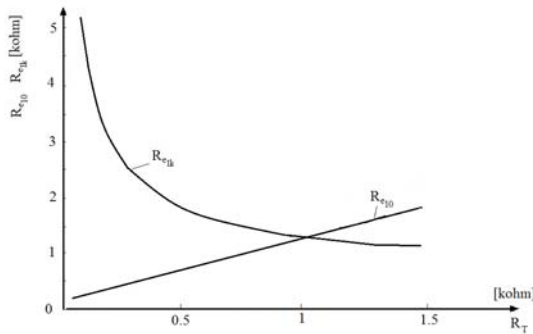


Figure 6. Characteristics  $R_{e10}(R_T)$ , and  $R_{e1k}(R_T)$  for the case (a)

Similarly, in Figure 7, the values of resistances  $R_{e10}(R_T)$ , and  $R_{e1k}(R_T)$  are graphically represented for the case b, when the two-port transfer parameters are not equal, based on the experimental results summarized in Table VI.

TABLE VI. EXPERIMENTAL VALUES OF THE EQUIVALENT RESISTANCE IN THE NO LOAD REGIME ( $R_{e10}$ ), AND THE EQUIVALENT RESISTANCE IN THE SHORT CIRCUIT ( $R_{e1k}$ ), DEPENDING ON THE TRANSVERSAL RESISTANCE ( $R_T$ ). FOR CASE (B)

$R_T$ [kΩ]	$U_1$ [V]	$I_{e10}$ [mA]	$I_{e1k}$ [mA]	$R_{e10}$ [kΩ]	$R_{e1k}$ [kΩ]
0.1	1.01	8.77	0.17	0.11	5.94
0.3	1.01	3.32	0.45	0.30	2.24
0.5	1.01	2.00	0.65	0.50	1.55
0.8	1.01	1.45	0.90	0.69	1.12
1	1.01	1.01	1.01	1.00	1.00
1.2	1.01	0.84	1.08	1.20	0.93
1.5	1.01	0.60	1.20	1.68	0.84

The equivalent circuit diagram becomes unidirectional for the same transfer resistance value as in case (a), that is,  $R_T = 1k\Omega$  (See Figure 7).

When a gyrator is ideal it is discernible that the transversal resistance ( $R_T$ ) is dependent on the equivalent resistance ( $R_{e10}$ ). This can be visualized in both analyzed cases (a, b) as a straight line crossing the origin.

The results obtained by PSpice simulation are displayed in Figure 8.

The value of the transfer resistance, which was experimentally determined, in the instance where the electrical diagram becomes unidirectional, corresponds to the value of this resistance obtained analytically and through numerical simulation PSpice.

The calculated data and the experimental results are

consistent each other, which implicitly confirms the hypothesis of counting as ideal the operational amplifiers in the analyzed diagram.

In fact, experimentally determined characteristics are practically overlapping the characteristics obtained analytically and through PSpice simulation.

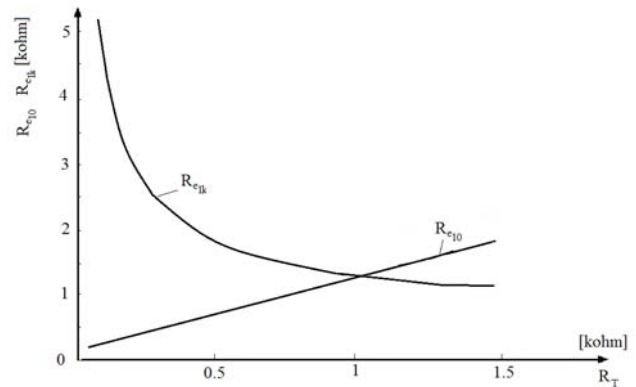


Figure 7. Characteristics  $R_{e10}(R_T)$ , and  $R_{e1k}(R_T)$  for the case (b)

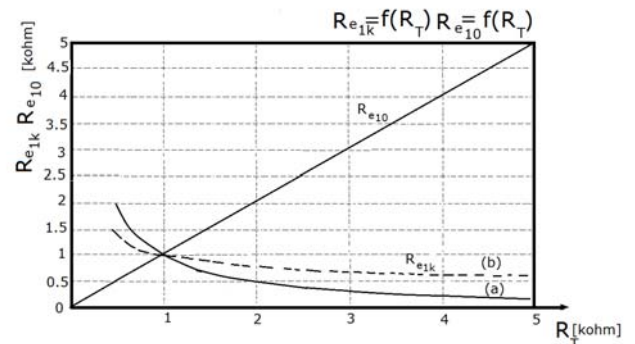


Figure 8. The dependence of the equivalent resistance in no-load ( $R_{e10}$ ), and equivalent resistances in short ( $R_{e1k}$ ), on the transversal resistance ( $R_T$ )

## VI. CONCLUSIONS

A two-port circuit is unidirectional if the energy is transferred in one direction only.

In a unidirectional two-port, where the transfer of electromagnetic power takes place only from ports 11' to 22', the chain matrix determinant is zero ( $|A|=0$ ) and the input impedance is independent of the load impedance. This entails that the conductance in no-load and short circuit conditions against both ports are equal to each other ( $G_{e10} = G_{e1k}$ ).

The unidirectional circuit necessary contains a gyrator and resistors connected transversal or longitudinal depending on the type of gyrator used.

The passive unidirectional two-port schemes can use Hall generator as gyrator component. In this type of unidirectional circuits, which entails a longitudinal resistance, the Hall gyrator acts as a lossy gyrator ( $G_{11} \neq 0, G_{22} \neq 0$ ).

When the gyrator component is an Antoniou operational amplifier, by an appropriate choice of resistors, the gyrator behaves as ideal ( $G_{11} = G_{22} = 0$ ). In this type of circuit, the resistance is transversally connected.

The unidirectional equivalent two-port circuit diagram built with operational amplifiers as gyrator structure was simulated in PSpice and verified experimentally.

The obtained results through the use of these two methods are consistent to each other and with the calculated ones.

Although the two cases (a, b) are different, the value of the transversal resistance ( $R_T$ ) is the same.

In the b case, the circuit diagram becomes unidirectional for the same transversal resistance value as in the case (a), that is,  $R_T=1k\Omega$ , which confirms experimentally the validity of the proposed circuit

The good agreement between obtained data validates that the studied circuit is unidirectional and permitted to consider the enclosed gyrator as ideal.

The main finding of paper is that this circuit with Antoniou operational amplifiers and transversal resistor behaves as unidirectional two-port. The advantage of this configuration is that it allows the use of an ideal gyrator in the structure of unidirectional circuits, improving the performance and increasing the energy transfer from a port to another. Due to high input impedance and low output impedance characteristics, gyrators with operational amplifiers may be used to implement transfer functions characteristics of active filter in a limited frequency spectrum.

#### REFERENCES

- [1] J. Zhai, J. Li, S. Dong, D. Viehland, M. I. Bichurin, "A Quasi (Unidirectional) Tellegen Gyrator," *Journal of Applied Physics*, vol. 100, no. 12, pp. 124509, 2006. doi:10.1063/1.2402967.
- [2] S. K. Mitra, "Equivalent Circuits of Gyrators," *Electronics Letters*, vol. 3, no. 7, p. 333, 1967. doi:10.1049/el:19670255.
- [3] J. Ou, M. F. Caggiano, "Determine Two-Port S-Parameters from One-Port Measurements Using Calibration Substrate Standards," *Proceedings Electronic Components and Technology*, vol. 2, pp.1765–1768, 2005. doi:10.1109/ectc.2005.1442034
- [4] M. Ehsani, I. Husain, M. O. Bilgic, "Power Converters as Natural Gyrators," *IEEE Transactions on Circuits and Systems*, vol. 40, no. 12, pp. 946–949, 1993. doi:10.1109/81.269036
- [5] T. Hasegawa, T. Okada, "Low Loss Lumped Element Isolator Using Gyrator Circuit With Two Asymmetrical Electrodes," *IEEE MTT-S International Microwave Symposium Digest*, pp. 540–543, 2006. doi:10.1109/mwsym.2006.249631.
- [6] F. Yuan, "CMOS Gyrator-C Active Transformers," *2007 IEEE International Symposium on Circuits and Systems*, pp. 3812 – 3815, May 2007. doi:10.1109/iscas.2007.378792
- [7] Y. Wang, J. Li, L.-X. Ran, "An Equivalent Circuit Modeling Method for Ultra-Wideband Antennas," *PIER*, vol. 82, pp. 433–445, 2008. doi:10.2528/pier08032303
- [8] M. Kagan, "On equivalent resistance of electrical circuits," *American Journal of Physics*, vol. 83, no. 1, pp. 53–63, 2015 doi:10.1119/1.4900918
- [9] A. Antoniou, "Realisation of gyrators using operational amplifiers, and their use in RC-active-network synthesis," *Proceedings of the Institution of Electrical Engineers*, London, vol. 116, no. 11, p. 1838, 1969. doi:10.1049/piee.1969.0339
- [10] L. Li, K. F. Han, X. Tan, N. Yan, H. Min, "Transconductance enhancement method for operational transconductance amplifiers," *Electronics Letters*, vol. 46, no. 19, p. 1321, 2010. doi:10.1049/el.2010.1575
- [11] A. Antoniou, "3-Port Gyrator Circuits Using Operational Amplifiers," *Electronics Letters*, vol. 4, no. 26, p. 591, 1968. doi:10.1049/el:19680461
- [12] A.-R. Ahmed, K.-W. Yeom, "An Extraction of Two-Port Noise Parameters From Measured Noise Powers Using an Extended Six-Port Network," *IEEE Trans. Microwave Theory Techn.*, vol. 62, no. 10, pp. 2423–2434, 2014. Online. Available: <http://dx.doi.org/10.1109/tmtd.2014.2345693>
- [13] D. Kouznetsov, "Superfunctions for amplifiers," *Optical Review*, vol. 20, no. 4, pp. 321–326, 2013. doi:10.1007/s10043-013-0058-6
- [14] A. Malcher, "Modified current differencing transconductance amplifier – new versatile active element," *Bulletin of the Polish Academy of Sciences: Technical Sciences*, vol. 60, no. 4, 2012. doi:10.2478/v10175-012-0085-7
- [15] K. Um, "Quantitative Analysis of Transmission Zeros in Cross-Coupled Two-Port Power Systems," *Japanese Journal of Applied Physics*, vol. 52, no. 10S, p. 10MB20, 2013. Online. Available: <http://dx.doi.org/10.7567/jjap.52.10mb20>
- [16] R. Y. Barazarte, G. G. Gonzalez, M. Ehsani, "Generalized Gyrator Theory," *IEEE Trans. Power Electron.*, vol. 25, no. 7, pp. 1832–1837, 2010. doi:10.1109/tpe.2010.2042820
- [17] G. Viola and D. P. DiVincenzo, "Hall Effect Gyrators and Circulators," *Physical Review X*, vol. 4, no. 2, 2014. doi:10.1103/physrevx.4.021019
- [18] S. Ghamari, G. Tasselli, C. Botteron, P.-A. Farine, "Design methodology for common-mode stability of OTA-based gyrators," *International Journal of Circuit Theory and Applications*, p. n/a–n/a, 2015. doi:10.1002/cta.2154.
- [19] Z. Liu, D. Chen, J. Ma, S. Wei, Y. Zhang, J. Dai, S. Liu, "Fast Algorithm of Discrete Gyrator Transform Based on Convolution Operation," *Optik - International Journal for Light and Electron Optics*, vol. 122, no. 10, pp. 864–867, 2011. doi:10.1016/j.ijleo.2010.06.010
- [20] Q. Wang, Q. Guo, L. Lei, "Double Image Encryption Based on Phase-Amplitude Mixed Encoding and Multistage Phase Encoding in Gyrator Transform Domains," *Optics & Laser Technology*, vol. 48, pp. 267–279, 2013. doi:10.1016/j.optlastec.2012.10.037
- [21] T. Mizoguchi, T. Nozaki, K. Ohnishi, "Examination of Stability and Characteristics of Gyrator Type Bilateral Control; Toward Controller and Transfer Impedance Design," *2012 5th International Conference on Human System Interactions*, 2012. doi:10.1109/hsi.2012.25
- [22] S. Singer, "Loss-Free Gyrator Realization," *IEEE Transactions on Circuits and Systems*, vol. 35, no. 1, pp. 26–34, 1988. doi:10.1109/31.1697
- [23] M.-C. Tsai, D.-W. Gu, "Two-Port Networks," *Advances in Industrial Control*, pp. 37–63, 2013. doi:10.1007/978-1-4471-6257-5\_3
- [24] G. Viola, D. P. DiVincenzo, "Hall Effect Gyrators and Circulators," *Physical Review X*, vol. 4, no. 2, May 2014. doi:10.1103/physrevx.4.021019
- [25] M. Onoda, N. Nagaosa, "Quantized Anomalous Hall Effect in Two-Dimensional Ferromagnets: Quantum Hall Effect in Metals," *Physical Review Letters*, vol. 90, no. 20, 2003. doi:10.1103/physrevlett.90.206601
- [26] H. Akera, "Hall-Potential Distribution in AC Quantum Hall Effect," *Journal of Physics: Conference Series*, vol. 334, p. 012019, 2011. doi:10.1088/1742-6596/334/1/012019
- [27] H. Chen, X. Du, Z. Liu, C. Yang, "Color Image Encryption Based on the Affine Transform and Gyrator Transform," *Optics and Lasers in Engineering*, vol. 51, no. 6, pp. 768–775, 2013. doi:10.1016/j.optlaseng.2013.01.016
- [28] Q. Zhang, T. Guo, B. A. Khan, T. Kodera, C. Caloz, "Coupling Matrix Synthesis of Nonreciprocal Lossless Two-Port Networks Using Gyrators and Inverters," *IEEE Trans. Microwave Theory Techn.*, vol. 63, no. 9, pp. 2782–2792, Sep. 2015. doi:10.1109/tmtd.2015.2450733
- [29] M. R. Abuturab, "Securing Color Information Using Arnold Transform in Gyrator Transform Domain," *Optics and Lasers in Engineering*, vol. 50, no. 5, pp. 772–779, 2012. doi:10.1016/j.optlaseng.2011.12.006
- [30] A. K. Nakamura, K. Hirota, "Equivalent Circuits for Unidirectional SAW-IDTs Based on the Coupling-of-Modes Theory," *IEEE Trans. Ultrason., Ferroelect., Freq. Contr.*, vol. 43, no. 3, pp. 467–472, 1996. doi:10.1109/58.489406
- [31] T. Mizoguchi, D. Yashiro, K. Ohnishi, "Experimental Evaluation of Transformer Gyrator Switching Bilateral Control," *IECON 2011 - 37th Annual Conference of the IEEE Industrial Electronics Society*, 2011. doi:10.1109/iecon.2011.6119373
- [32] Liu, L. Xu, Q. Guo, C. Lin, S. Liu, "Image Watermarking by Using Phase Retrieval Algorithm in Gyrator Transform Domain," *Optics Communications*, vol. 283, no. 24, pp. 4923–4927, 2010. doi:10.1016/j.optcom.2010.07.034